Int J Clin Exp Med 2016;9(2):3586-3592
www.ijcem.com /ISSN:1940-5901/IJCEM0016302

Original Article

Correlation between imageological characteristics and pathological patterns of mini-nodule lung cancer

Hai-Yun Ren[1], Peng Ji[2], Liu Liu[1], Wei Yan[1], She-Tian Jiang[1]

[1]*Department of Ultrasound, Zhumadian Central Hospital, Zhumadian, China;* [2]*Department of Radiotherapy, Zhumadian Central Hospital, Zhumadian, China*

Received July 9, 2015; Accepted January 7, 2016; Epub February 15, 2016; Published February 29, 2016

Abstract: This study aims to explore the relationship between the imageological characteristics and the pathological patterns in patients with mini-nodule lung cancer, and to investigate the threshold value for predicating the pathological patterns with invasive characteristic from the imageological aspect. A total of 137 lung cancer patients were selected to record the characteristics of the maximum diameter, density, blood-supply, vacuole and mini-lobules and analyze their relationships with pathological patterns. Receiver Operating Characteristic (ROC) analysis was applied to predicate the threshold value of lung cancer invasiveness. There were significant differences in the maximum diameter, density, blood supply, sublobe, burr and pleural indentation syndrome of the nidi in lung cancer patients with different pathological patterns ($P<0.05$ or $P<0.01$). Further analysis on the relationships between the above characteristics and lung cancer invasiveness showed that lung cancer invasiveness was in moderate correlation with the nodular density (r=0.589, P=0.000), in low connection with nodular size (r=0.368, P=0.000) and in extremely weak association with blood supply, sublobe, burr and pleural indentation syndrome ($r<0.3$). ROC analysis on the nodular size and density indicated that the area under ROC curve, sensitivity and specificity of nodular size were 0.700, 0.861, and 0.431 respectively, with threshold value being 12.50 mm, while those of nodular density were 0.831, 0.806 and 0.769, with threshold value being 37.50%, respectively. Imageological characteristics, especially the nodular size and density, have certain predictable value in the invasiveness of mini-nodule lung cancer.

Keywords: Lung cancer, lung nodule, imageological characteristics, pathological pattern

Introduction

Lung cancer, which is also called bronchial lung cancer because most of it is derived from the bronchial epithelium, is a kind of malignant tumor with the highest morbidity across the whole world [1, 2]. Because of the absence of specific clinical manifestation in the early stage of lung cancer and effective early diagnostic methods, 80% patients are in middle and advanced stage when diagnosed, thus leading to huge therapeutic cost but slight survival benefits [3]. It was reported that lung cancer-related death accounted for 23.8% of all cancer-associated death, and the 5~10-year survival rate of patients with lung cancer was only 8~14% [4]. In another study, the 5-year survival rate of the patients with lung cancer received early diagnosis and treatment was increased from 14% to 49%, which was even >70% in stage I A patients, and if treatment could be given in the early micro-damage of primary cancer, the recovery rate could be up to 100% [5]. Therefore, the early detection and cognition of lung cancer is of critical significance in improving the patients' survival rate [6].

Early lung cancer is usually represented by lung nodules that are defined as the round or quasi-circular dense regions with diameter ≤30 mm in lung parenchyma [7]. At present, the primary methods for the diagnosis of lung nodules include various imageological methods such as X-ray and computed tomography (CT), etc. However, due to the complex structure of lung, different shapes and sizes of lung nodules and the similarities of CT value of lung nodules to that of some other lung tissues, the early or smaller nodular nidi can be easily confused when being overlapped with the vascular images, thus leading to the difficulty in finding the lung nodules and resulting in the subjective and

objective misdiagnosis. In recent years, with the continuous update and improvement of CT devices, imaging software and scanning techniques, the accuracy and reliability are significantly promoted, especially the popularization of low-dose spiral CT that markedly increases the detection rate of lung nodules, the mini-nodules in particular [8]. To further distinguish the property of lung nodules, analyze the relationships between the morphological characteristics of mini-nodule nidi and the pathological patterns and to seek a reliable threshold value to predicate the low- and high-invasiveness lung cancer, this study diagnosed the imageology of patients with lung cancer and compared them with the pathological diagnostic results.

Materials and methods

General data

This study was approved by the Ethnic Committee of Zhumadian Central Hospital and all informed consent forms were signed by the patients and (or) their families. A total of 137 patients with lung cancer admitted in Zhumadian Central Hospital from October, 2009 to February, 2015 were selected as study objects. All patients were diagnosed as non-small cell lung cancer (NSCLC) and treated with surgical resection. The lung nodules ≤20 mm and all patients had complete CT thin-layer three-dimensional imageological data before operation. There were 91 males and 46 females; aged 34~79 years, with median age of 57 years; clinical stage: 129 in stage I, 2 in stage II and 6 in stage III; 4 were with atypical adenomatous hyperplasia (AAH), 39 with adenocarcinoma insitu (AIS), 22 with microinvasive adenocarcinoma (MIA), 68 with invasive adenocarcinoma (IAC), 3 with squamous (SQ) and 1 with large cell carcinoma (LC); 69 with single nidus and 68 with multiple nidi; and 12 were with multiple primary tumor.

Methods

Siemens 64-layer high-resolution spiral CT was used to perform thin scanning (1 mm) before operation and re-construct three-dimension. According to the pre-established image-reading sequence, the maximum diameter, density, blood supply, vacuole, mini-nodules, morphology, sublobe, burr, pleural indentation syndrome and the presence of multiple nidi were recorded. The images were read jointly by 2 chief physicians from Department of Internal Medicine, 2 from Department of Radiotherapy and 1 from Department of Pathology who were unknown of the pathological results.

Evaluation criteria

The maximum diameter of nidi was defined as the maximum diameter of the measuring nidi on the maximum plane and was then divided into 3 grades (≤10 mm, 10~15 mm and 15~20 mm). Nodular density was defined as the ratio of parenchymal component in the mini-nodular lesion and divided into 5 grades (0%: pure ground-glass opacity; 100%: pure parenchymal nodules; 25%, 50% and 75%: the ratio of parenchymal component accounted for 25%, 50% and 75%, respectively). Mini-nodules were the regional clustered granules with increased density in nodules. Round and quasi-circular forms were defined as regular morphology and others as irregular morphology. Sublobe was defined as the nodule border with obvious depression. Multiple nidi meant there were multiple nodular nidi in the lung, including benign and malignant lesions and nidi with unknown property. AAH, AIS and MIA were defined as low-invasiveness lung cancer while IAC, LC and SQ as high-invasiveness lung cancer.

Statistical analysis

SAS 9.3 and SPSS 17.0 were applied for all data analysis. Enumeration data was expressed by percentage (%) and detected with χ^2 test. The relationship between invasiveness and imageological characteristics was analyzed by Spearman correlation analysis and Receiver Operating Characteristic (ROC) was used to analyze the optimal diagnostic threshold value.

Results

Relationships between imageological characteristics and pathological patterns in lung cancer

Of the 137 patients, there were 151 mini-nodules with imageological and pathological results. AAH and AIS were marked by pure ground-glass nodules in round or quasi-circular shape, with clear broader; MIA was manifested by pure ground-glass nodules or density-mixed

Figure 1. Comparison of imageological characteristics of mini-nodule lung cancer with different pathological patterns. Note: A: IAC, imageology showed mixed ground-glass nodular images; B: MIA, imageology showed ground-glass ingredient-based partial parenchymal nodules, and the parenchymal ingredients were located in the center of the lesions; C: AIS, imageology showed pure ground-glass nodular images.

Table 1. Relationships between pathological patterns and imageological characteristics of mini-nodule lung cancer

Imageological characteristics	Pathological results [N (%)]					X^2	*P*
	AAH	AIS	MIA	IAC	Non-adenocarcinoma		
The maximum diameter							
≤10	4 (3.93)	15 (52.94)	9 (18.58)	10 (2.857)	0 (0)	31.4802	0.0017
10~15	0 (0)	17 (31.48)	8 (14.81)	28 (51.85)	1 (1.85)		
15~20	0 (0)	7 (15.56)	5 (11.11)	30 (66.67)	3 (6.67)		
Density							
0%	3 (8.33)	24 (66.67)	4 (11.11)	5 (13.89)	0 (0)	78.2325	<0.0001
25%	1 (3.57)	9 (32.14)	9 (32.14)	9 (32.14)	0 (0)		
50%	0 (0)	3 (20.00)	3 (20.00)	9 (60.00)	0 (0)		
75%	0 (0)	2 (11.11)	1 (5.56)	15 (83.33)	0 (0)		
100%	0 (0)	1 (2.50)	5 (12.50)	30 (75.00)	4 (10.00)		
Blood supply							
Clinging to the periphery of nodular vessels	3 (13.04)	11 (47.83)	3 (13.04)	6 (26.09)	0 (0)	14.9767	0.0047
Entering into nodular vessels	1 (0.88)	28 (24.56)	19 (16.67)	62 (54.39)	4 (3.51)		
Vacuole syndrome							
No	3 (3.19)	25 (26.60)	15 (15.96)	46 (48.94)	4 (4.26)	3.4497	0.4856
Yes	1 (2.27)	14 (31.82)	7 (15.91)	22 (50.00)	0 (0)		
Mini-nodule							
No	3 (3.09)	28 (28.87)	17 (17.53)	45 (46.39)	4 (4.12)	3.9682	0.4103
Yes	1 (2.50)	11 (27.50)	5 (12.50)	23 (57.50)	0 (0)		
Morphological regulation							
No	2 (3.51)	13 (22.81)	10 (17.54)	31 (54.39)	1 (1.75)	2.2964	0.6814
Yes	2 (2.50)	26 (32.50)	12 (15.00)	37 (46.25)	3 (3.75)		
Sublobes							
No	3 (6.98)	16 (37.21)	8 (18.60)	16 (37.21)	0 (0)	10.1292	0.0383
Yes	1 (1.06)	23 (24.47)	14 (14.89)	52 (55.32)	4 (4.26)		
Burr							
No	4 (4.00)	35 (35.00)	13 (13.00)	44 (44.00)	4 (4.00)	15.9748	0.0031
Yes	0 (0)	4 (10.81)	9 (24.32)	24 (64.86)	0 (0)		
Pleural indentation syndrome							
No	3 (3.61)	29 (34.94)	16 (19.28)	32 (38.55)	3 (3.61)	10.5221	0.0325
Yes	1 (1.85)	10 (18.52)	6 (11.11)	36 (66.67)	1 (1.85)		
Multiple nodules							
No	1 (1.45)	19 (27.54)	9 (13.04)	38 (55.07)	2 (2.90)	2.7395	0.6023
Yes	3 (4.41)	20 (29.41)	13 (19.12)	30 (44.12)	2 (2.94)		

Table 2. Relationships between imageological characteristics and mini-nodule lung cancer invasiveness

Imageological characteristics	Pathological results [*n* (%)]		*r*	*P*
	Low invasiveness	High invasiveness		
Maximum diameter				
≤10a	28 (87.95)	10 (12.45)	0.368	0.000
10~15	25 (46.30)	29 (53.70)		
15~20	12 (26.67)	33 (73.33)		
Density				
0%	31 (86.11)	5 (13.89)	0.589	0.000
25%	19 (67.86)	9 (32.14)		
50%	6 (40.00)	9 (60.00)		
75%	3 (16.67)	15 (83.33)		
100%	6 (15.00)	34 (85.00)		
Blood supply				
Clinging to the periphery of nodular vessels	17 (73.91)	6 (26.09)	0.238	0.005
Entering into nodular vessels	48 (42.11)	66 (57.89)		
Sublobe				
No	27 (62.79)	16 (37.21)	0.208	0.015
Yes	38 (40.43)	56 (59.57)		
Burr				
No	52 (52.00)	48 (48.00)	0.150	0.080
Yes	13 (35.14)	24 (64.86)		
Pleural indentation syndrome				
No	48 (57.83)	35 (42.17)	0.258	0.002
Yes	17 (31.48)	37 (68.52)		

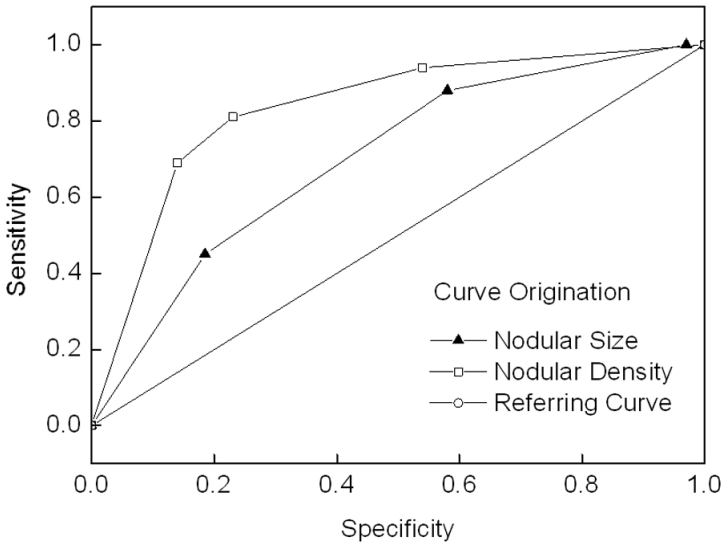

Figure 2. ROC curve of nodular size and density in diagnosis of mini-nodule lung cancer.

ground-glass nodules in round or quasi-circular shape, with clear broader; and IAC was mostly defined as density-mixed ground-glass nodules with irregular shapes. χ^2 test showed that from AAH, AIS and MIA to IAC, the maximum diameter, density, sublobe, burr, pleural indentation syndrome and the ratio of blood supply entering into nodular vessels increased subsequently, and there were significant differences ($P<0.05$ or $P<0.01$). The comparison of imageological diagnosis and pathological patterns are shown in **Figure 1** and **Table 1**.

Relationships between imageological characteristics and mini-nodule lung cancer invasiveness

Further analysis on the relationships between the above indexes and lung cancer invasiveness showed that lung cancer invasiveness was in moderate correla-

Table 3. ROC related parameters of nodular size and density in diagnosis of mini-nodule lung cancer

	AUC	Sensitivity	Specificity	Threshold value	P	95% CI
Nodular size	0.700	0.861	0.431	12.50 mm	<0.05	0.612-0.788
Nodular density	0.831	0.806	0.769	37.50%	<0.05	0.760-0.902

tion with the nodal density, in low connection with nodular size and in extremely weak association with blood supply, sublobe, burr and pleural indentation syndrome (**Table 2**).

Diagnostic value of nodal size and density in mini-nodule lung cancer

ROC analysis on the nodular size and density indicated that the area under ROC curve, sensitivity and specificity of nodular size were 0.700 (95% CI; 0.612~0.788), 0.861, and 0.431, with threshold value being 12.50 mm, while those of nodular density were 0.831 (95% CI: 0.760~0.902), 0.806 and 0.769, with threshold value being 37.50%, respectively (**Figure 2** and **Table 3**). The area under the ROC curve is a popular summary measure of the accuracy of a test. Since the area under ROC curve of nodular density was higher than nodular size, nodal density had higher predictable value in the invasiveness of mini-nodule lung cancer.

Discussion

With the development of CT imageological technique, the detection rate of mini-nodules in lung has been significantly increased. According to the clinical statistics, the detection rate of nodular lesion by conventional chest X-ray was 0.2%, but was 40%~60% by high-resolution CT [9]. Dabrowska *et al.* [10] applied contrast-enhancement CT and 18-FDG positron emission computed tomography (PECT) to identify the malignant isolated lung nodules, in which the optimal diagnostic point of contrast-enhancement CT was 19 hounsfield units of enhancement value, whose sensitivity, specificity, positive predictive value (PPV), negative predictive value (NPV) and accuracy were 100%, 37%, 32%, 100% and 58% respectively, whereas on the optimal diagnostic point of 18-FDG PECT, the sensitivity, specificity, PPV, NPV and accuracy were 77%, 92%, 83%, 89% and 90% respectively, showing that the two had their own advantages and disadvantages in sensitivity and specificity. Altenbernd *et al.* [11] used dual-energy CT to scan the patients with tumor metastases, whose results demonstrated that a total of 156 lung nodules with the maximum diameter ≥5 mm were found, and the measured CT value of lung nodules could be applied for distinguishing the primary tumors.

Early detection and intervention are of great significance in reducing the mortality of patients with lung cancer [12, 13]. American *National Lung Screening Trial* (NLST) has proved that low-dose spiral CT examination once a year can greatly reduce the relevant death risk by 20% in high-risk patients with lung cancer [14]. It was illustrated in a study that AAH, AIS and MIA were tumors with favorable prognosis in adenocarcinoma, which showed scale-like growth or mainly in scale-like growth, with tumor size ≤3 cm and postoperative survival rate near to 100% after radical surgery, whereas IAC was mainly in scale-like, acinar, palillary and solid growth, and the 5-year survival rate of IAC patients with stage I was 70%~80%, with evidently lower prognosis than that of AIS and MIA [15]. Therefore, preoperative effective diagnosis of the risk of mini-nodule lung cancer, which can guide the physicians to conduct different interventional measures, is of great significance in clinic. However, due to the facts that there lacks gold standard for the diagnosis in clinic and the emphasis of the previous studies is on the differentiation of benign and malignant nodules, the difference between mini-nodule lung cancer is ignored, thus leading to the deficiency or excess of interventions in clinic [16].

This study analyzed the relationships between the CT imageological characteristics and pathological patterns in patients with mini-nodule lung cancer, aiming to use imageological characteristics to reflect the lung cancer subtypes with high-invasiveness. The results of this study revealed that the imageological characteristics changed in mini-nodule lung cancer patients with different pathological patterns, especially in adenocarcinoma subtypes, and the maxi-

mum diameter and density of mini-nodules increased along with the aggravation of infiltration severity, indicating that the size and density of mini-nodules might reflect the developmental process of lung cancer. Additionally, although blood supply, sublobe, burr and pleural indentation syndrome were in weak association with lung cancer invasiveness, there was no significant difference in different pathological patterns, which could provide references for the diagnosis of the pathological patterns of mini-nodule lung cancer. In this study, ROC analysis was applied to further analyze the size and density of nodules related to moderate and poor differentiation, whose results demonstrated that as to highly-suspected mini-nodules in clinic, if the maximum diameter was >12.50 mm and the ratio of parenchymal component in ground-glass opacity was 37.50%, the patient could be diagnosed as high-invasiveness lung cancer.

To sum up, if the size and density of mini-nodules reached to the optimal diagnostic points and one of the imageological characteristics (blood supply, sublobe, burr and pleural indentation syndrome) was accompanied, the patients could be diagnosed as high-invasiveness lung cancer, for which positive interventional measures, like standard radical surgery was recommended. And if the above conditions were not achieved, surgical method should be further studied to reduce the range of surgical resection and avoid excessive intervention.

Acknowledgements

This research received no specific grant from any funding agency in the public, commercial, or not-for-profit sectors.

Disclosure of conflict of interest

None.

Address correspondence to: Hai-Yun Ren, Department of Ultrasound, Zhumadian Central Hospital, No. 747 Zhonghua Road, Zhumadian 463000, Henan, China. Tel: +86-13583578692, E-mail: renhaiyun15915@163.com

References

[1] Zhang Y, Yu LK and Xia N. Effect of brucea javanica oil emulsion combined with GP regimen on the immune function of patients with advanced non-small cell lung cancer. J Int Transl Med 2014; 2: 262-265.

[2] Shen D and Li CH. The influence of compound shougong powder on JAK2-STAT3 signaling pathway in mice with lewis lung cancer. J Int Transl Med 2014; 2: 476-481.

[3] Yan Y, Zhang YX, Fang WF, Kang SY, Zhan JH, Chen N, Hong SD, Liang WH, Tang YN, He DC, Wu X and Zhang L. Roles of immunohistochemical staining in diagnosing pulmonary squamous cell carcinoma. Asian Pac J Cancer Prev 2015; 16: 551-557.

[4] Ma L, Wu H and Sun J. The expression of ezrin and its significance in non-small cell lung cancer. J Int Transl Med 2014; 2: 408-412.

[5] Lee HY, Choi YL, Lee KS, Han J, Zo JI, Shim YM and Moon JW. Pure ground-glass opacity neoplastic lung nodules: histopathology, imaging, and management. AJR Am J Roentgenol 2014; 202: W224-233.

[6] Wang HQ, Zhao L, Zhao J and Wang Q. Analysis on early detection of lung cancer by PET/CT Scan. Asian Pac J Cancer Prev 2015; 16: 2215-2217.

[7] Lee HY and Lee KS. Ground-glass opacity nodules: histopathology, imaging evaluation, and clinical implications. J Thorac Imaging 2011; 26: 106-118.

[8] Nagatani Y, Takahashi M, Murata K, Ikeda M, Yamashiro T, Miyara T, Koyama H, Koyama M, Sato Y, Moriya H, Noma S, Tomiyama N, Ohno Y, Murayama S; investigators of ACTIve study group. Lung nodule detection performance in five observers on computed tomography (CT) with adaptive iterative dose reduction using three-dimensional processing (AIDR 3D) in a Japanese multicenter study: Comparison between ultra-low-dose CT and low-dose CT by receiver-operating characteristic analysis. Eur J Radiol 2015; 84: 1401-1412.

[9] Kim HY, Shim YM, Lee KS, Han J, Yi CA and Kim YK. Persistent pulmonary nodular ground-glass opacity at thin-section CT: histopathologic comparisons. Radiology 2007; 245: 267-275.

[10] Dabrowska M, Krenke R, Korczynski P, Maskey-Warzechowska M, Zukowska M, Kunikowska J, Orłowski T and Chazan R. Diagnostic accuracy of contrast-enhanced computed tomography and positron emission tomography with 18-FDG in identifying malignant solitary pulmonary nodules. Medicine (Baltimore) 2015; 94: e666.

[11] Altenbernd J, Wetter A, Umutlu L, Hahn S, Ringelstein A, Forsting M and Lauenstein T. Dual-energy computed tomography for evaluation of pulmonary nodules with emphasis on metastatic lesions. Acta Radiol 2015; [Epub ahead of print].

[12] Wu XY and Huang XE. Screening for patients with non-small cell lung cancer who could survive long term chemotherapy. Asian Pac J Cancer Prev 2015; 16: 647-652.
[13] Veronesi G. Lung cancer screening: the european perspective. Thorac Surg Clin 2015; 25: 161-174.
[14] National Lung Screening Trial Research Team, Aberle DR, Adams AM, Berg CD, Black WC, Clapp JD, Fagerstrom RM, Gareen IF, Gatsonis C, Marcus PM and Sicks JD. Reduced lung-cancer mortality with low-dose computed tomographic screening. N Engl J Med 2011; 365: 395-409.
[15] Liu H, Zhang CM, Su ZY, Wang K and Deng K. Research on a pulmonary nodule segmentation method combining fast self-adaptive FCM and classification. Comput Math Methods Med 2015; 2015: 185726.
[16] Lee SM, Park CM, Goo JM, Lee HJ, Wi JY and Kang CH. Invasive pulmonary adenocarcinomas versus preinvasive lesions appearing as ground-glass nodules: differentiation by using CT features. Radiology 2013; 268: 265-273.